Building and Environment 59 (2013) 436–447

Contents lists available at SciVerse ScienceDirect

Building and Environment

journal homepage: www.elsevier.com/locate/buildenv

Bioaerosol deposition in single and two-bed hospital rooms: A numerical and experimental study

M.-F. King*, C.J. Noakes, P.A. Sleigh, M.A. Camargo-Valero

Pathogen Control Engineering Institute, School of Civil Engineering, University of Leeds, Leeds LS2 9JT, UK

ARTICLE INFO

Article history:
Received 6 June 2012
Received in revised form
8 September 2012
Accepted 16 September 2012

Keywords:
Hospital acquired infection
Particle deposition
CFD
Turbulence models
Experiment
Bioaerosol

ABSTRACT

Aerial dispersion of pathogenic microorganisms and subsequent contamination of surfaces is well recognised as a potential transmission route for hospital acquired infection. Simulation approaches such as computational fluid dynamics (CFD) are increasingly used to model particle behaviour in indoor air and the results interpreted to infer infection risk. However there is little validation of such methods in the open literature. This paper considers the ability of CFD simulations to accurately predict spatial distributions of bioaerosol deposition in indoor environments and explores the influence that different room layouts have on deposition patterns. Spatial deposition of aerosolised *Staphylococcus aureus* was measured in an aerobiology test room arranged in three different layouts: an empty room, a single-bed and a two-bed hospital room. Comparison with CFD simulations using Lagrangian particle tracking demonstrates that a realistic prediction of spatial deposition is feasible, and that a Reynolds Stress (RSM) turbulence model yields significantly better results than the $k-\varepsilon$ RNG turbulence model used in most indoor air simulations. Results for all layouts demonstrate that small particle bioaerosols are deposited throughout a room with no clear correlation between relative surface concentration and distance from the source. However, a physical partition separating patients is shown to be effective at reducing cross-contamination of neighbouring patient zones.

1. Introduction

The risk of acquiring nosocomial infections is omnipresent in health-care facilities worldwide. Globally it is estimated that 1.4 million people are suffering from such an affliction at any one time [1]. In the USA for example, the National Nosocomial Infections Surveillance (NNIS) calculated that approximately 1.7 million patients were infected by Healthcare Associated Infections (HCAIs) and 99,000 attributable deaths were reported in 2002 [2]. The European counterpart (Hospital in Europe Link for Infection Control through Surveillance – HELICS) considers the figure of affected patients to be around 5 million in Europe [1]. Differences in benchmarking of surveillance data often make comparisons difficult on an international level however the significance of the problem is undisputed. While the transmission routes for some diseases are well documented, the precise mode of transmission is uncertain for many infections, particularly for those pathogens that cause HCAIs. Although it is highly likely that the majority of transmission occurs via a contact route [1], there is evidence suggesting that at least 20% of HCAIs potentially could have arisen from an environmental reservoir [3].

Deposition of pathogen laden bioaerosols has been highlighted as a potential mechanism for such environmental contamination. Several recent studies have demonstrated a strong correlation between hospital airborne microflora and contaminated surfaces [4,5]. Complementary studies have shown that the application of air cleaning technologies can reduce surface contamination [6]; while others have highlighted that environmental contamination, through the deposition on surfaces, cannot be underestimated in the contribution to fomite-based transmission [7–9]. That said, the fate of aerial pathogens in indoor environments is still poorly understood and constitutes an area of much controversy and challenging research. Conventional infection theory regards bioaerosol particles with a diameter below 5 μm (e.g., droplet nuclei) as remaining airborne and being controlled by ventilation, while particles with larger diameters (e.g., larger droplets from a sneeze, skin squama, etc) are cited as depositing out of the air within a 2 m radius of the source [10,11]. However the reality is not quite so clear cut. Smaller particles, while remaining airborne for longer, may still deposit out onto surfaces creating a possible contact transmission risk. While very large particles (>100 μm) will clearly deposit quickly, mid-range (5–100 μm) particles will be influenced by the air, initially

* Corresponding author. Tel.: +44 113 343 3292; fax: +44 113 343 2265.
E-mail address: bs07mfk@leeds.ac.uk (M.-F. King).

0360-1323/$ – see front matter © 2012 Elsevier Ltd. All rights reserved.
http://dx.doi.org/10.1016/j.buildenv.2012.09.011

through evaporation and then subsequently by ventilation flow patterns [12,13]. As a result, the final destination of an airborne pathogen may be many metres away from its original source.

Understanding the role that ventilation airflow and ward design play in the dispersion and deposition of infectious bioaerosols is tantamount to assessing pathogen exposure risk. With the difficulties in aerosolising microorganisms in most experimental settings, many studies have turned to inert particle tracers [14,15] or computational fluid dynamics (CFD) models to infer bioaerosol behaviour in air and deposition onto surfaces [16]. As highlighted by Hathway et al. [17] direct comparison between CFD models and bioaerosol experiments is sparse. Wong et al. [18] undertook a small scale experimental/numerical comparison using bioaerosol deposition within a climatically controlled enclosure. They showed good comparison using the RNG $k-\varepsilon$ turbulence model and their results are encouraging at high grid densities, despite the many reservations held regarding eddy viscosity turbulence modelling. Hathway et al.'s study [17] is the only direct comparison between measured airborne concentrations and CFD simulations in a controlled room scale environment. While they also analysed and modelled deposition on the floor of an empty test room, only total deposition was considered and hence spatial variation is still uncharacterised. Lai and Chen [19,20] predicted deposition of particles sizes ranging from 0.01 to 10 μm with strong evidence supporting the claim that larger particles drop close to the source and do not remain suspended.

Deposition of bioaerosols also has implications for ward layout. Recommended bed spacing in multi-bed environments is often cited as being based on droplet transmission risk [21], and studies have recognised the relevance for pathogens such as *Staphylococcus aureus* as well as respiratory diseases [22]. Tracer gas and simulation studies have shown that ventilation design [13,23] and the presence of partitions between beds [23] influences airborne cross-infection risk between two patients. Several studies advocate the benefits of single patient rooms in reducing infection risk [24–26], although it is difficult to ascertain whether benefits can be directly attributed to room design or resulting change in nursing and hygiene practice. In reality many hospitals are constrained by their existing building stock and have a shortage of single rooms. There is currently little knowledge as to the importance of bioaerosol deposition in environmental contamination, so quantifying deposition in both single and multi-bed rooms is important for informing nursing practice and design.

This study uses a combined experimental and CFD modelling approach to evaluate the spatial distribution of bioaerosol deposition in a ventilated room. The primary objective of the study is to demonstrate, under a full-scale test environment, that CFD simulations are able to predict realistic deposition patterns for small diameter bioaerosol particles. The secondary objective of the study is to establish the influence of room layout on the spatial deposition of bioaerosols and the implications for infection control in a hospital context. The work builds on that of Hathway et al. [17] to carry out a direct comparison between the deposition pattern of a non-fastidious microorganism (*S. aureus*) nebulised into an aerobiology test room and the predicted deposition from CFD models incorporating Lagrangian particle tracking methodologies and two alternative turbulence models. The study then considers idealised single and two-bed hospital room scenarios to explore how the location of the source and room and ventilation layout influences the relative deposition on key surfaces in a patient environment.

2. Experimental methodology

2.1. Experimental set-up

Experiments were conducted in the environmentally controlled, negatively pressurized, aerobiology chamber at the University of Leeds. Dimensions are close to a hospital single room: 4.26 m (L) × 3.36 m (W) × 2.26 m (H). All walls are well insulated and considered adiabatic. External air was HEPA filtered before being conditioned by a humidifier and heater. This air was supplied to the chamber through a high level wall mounted diffuser as shown in Fig. 1.

Extraction of air was at a low-level, diagonally opposite; through a grille of the same design (Outlet). The ventilation rate in all experiments was 6 ACH, verified by using a balometer (Model PH721, TSI Incorporated, Shoreview, MN). Inlet air temperature (21.8 °C ± 1 °C) and humidity (60% ± 7%) were controlled throughout the experiments.

Prior to conducting bioaerosol experiments, air velocities in the empty room were measured using a hot wire comfort anemometer (Testo Ltd, Germany. Accuracy: ±0.01 m/s). Measurements were made on vertical lines at 5 selected locations in the room and at the supply air diffuser. The diffuser velocity profile (Fig. 1) was used to generate suitable boundary conditions for the CFD model, while the in-room measurements were for CFD validation purposes. Four main experimental scenarios were investigated as summarised in Table 1.

Empty room: The first experiment is similar to Hathway et al. [17], quantifying the spatial distribution of deposition in a similar manner to Wong et al. [18] but at a room-scale. Bioaerosol injection occurred at the geometric centre point in the room and no furniture or heat sources were present.
Single room: Experimental set-up number two replicates the situation within a single-bed, hospital room, where an infectious patient lies resting. A heated mannequin (DIN-man) is used to represent the heat source of the human. Particle collection is made on surfaces which mimic hospital furniture.
Double room: Scenarios three and four both present two heated mannequins, employed in a similar manner to Qian et al. [13]. Cross contamination of surfaces surrounding an infectious and a susceptible patient is examined by the collection of bioaerosols on adjacent surfaces. The effect of ventilation is investigated by reversing the location of susceptible and infectious source. The effect of a partition between the two beds is also included.

In scenarios 2–4, a quiescent patient was simulated by a DIN man (Deutsche Institut für Normung), a hollow aluminium cylinder (length 1 m by diameter 0.35 m) with an interior heat source. The heat source was created by a 100 W light bulb to represent the thermal emission of a resting adult human. Convective heat output from the skin is considered to be approximately 50%. Dimensions of the cylinder are however smaller than the average person but emit a similar heat flux. Infra-red thermal imaging of the DIN man shows the surface temperature in Fig. 2, which represents approximate body equivalents.

2.2. Bioaerosol generation

Staphylococci are spherical gram positive bacteria existing endogenously on most human skin squamae. With shedding of $\sim 10^6$ skin flakes per day, they are consequently abundant in many health-care settings [17,18]. *S. aureus* was chosen as the bacteriological agent given its ability to grow on general purpose media with ease. The *S. aureus* culture was incubated in nutrient broth (Oxoid, UK) for 24 h at 37 °C. Subsequent dilution tests showed the nebuliser concentration to be circa 10^{11} organisms per ml. A 10 ml aliquot of the pure culture was aseptically removed and suspended in 100 ml of sterile distilled water in a pre-autoclaved nebuliser. Sterile distilled water was the preferred suspension medium since it did not produce foaming of the suspension during nebulisation.

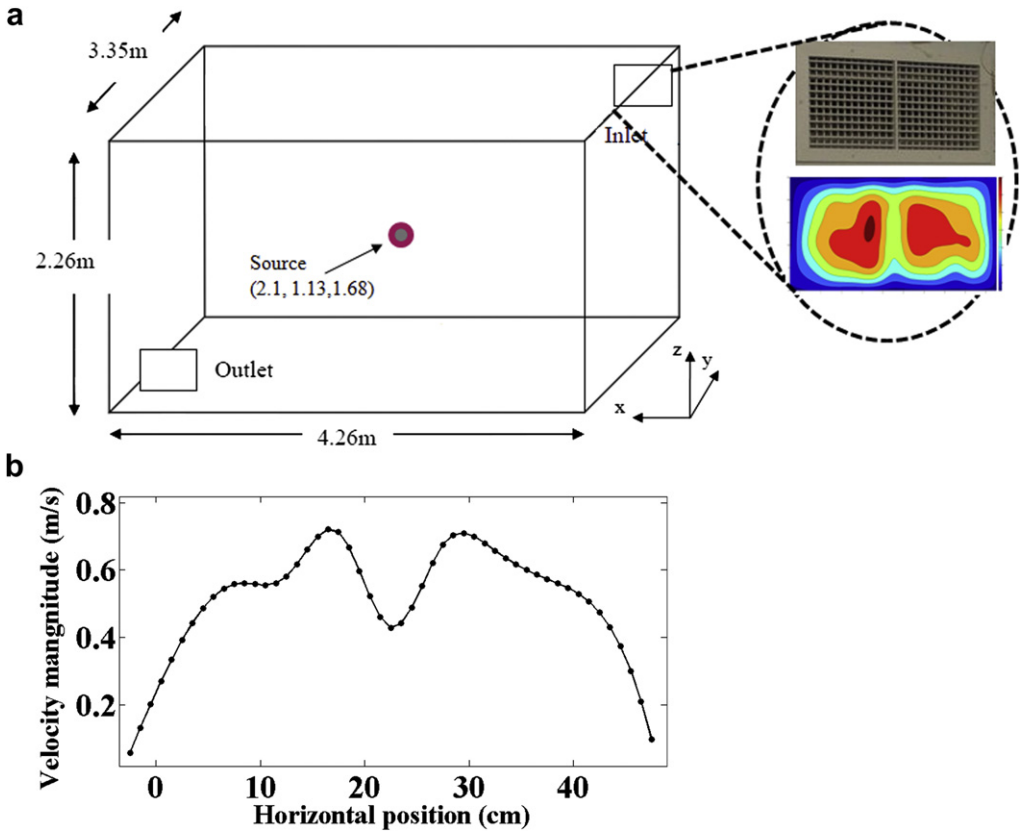

Fig. 1. Chamber geometry including centreline air speeds at the inlet. (a) Chamber geometry including source location for scenario 1 (Table 1) and contour plot showing measured velocities at inlet diffuser: (range: 0–0.7 m/s). (b) Horizontal centreline plot of velocity magnitudes measured at the inlet diffuser.

Aerosols were injected into the room via a six jet Collison Nebuliser (CN 25, BGI Inc, USA) attached to the inlet port of the chamber. The nebuliser utilises a separate pump, pressure regulator and metre operating at a flow rate of 8 L min^{-1} to deliver HEPA filtered air. Manufacturer's data from BGI indicate the size distribution of particles ejected during the process to have a mean mass diameter of 2.5 μm and a standard deviation of 1.8 μm. Eventual size distribution may vary through evaporation and the experimental set-up. While bioaerosol samples were not taken here, previous studies such as Hathway [4] have shown this experimental approach typically results in a bioaerosol concentration in the room of the order of 10^3–10^4 cfu/m^3, with over 90% of the bioaerosols collected on plates 5 and 6 of an Anderson sampler, corresponding to particle diameters of the order 1–2 μm (Anderson 1958). Method of injection varied based on the requirements for each experimental scenario. In the case of the empty chamber (scenario 1), bioaerosols were released from the centre of the room isotropically. In subsequent cases, (scenarios 2–4) a plastic tube of 2.5 cm Ø was clamped at the head of the infectious DIN-man and droplets were released into the thermal plume.

Table 1
Experimental scenarios. *Heated cylinders (DIN man) used as mannequins to produce a thermal plume representative of a human.

Case N°	1	2	3a 3b	4a 4b
Scenario	Empty room	Single room	Double room no partition	Double room with partition
Details	No furniture or mannequin	Hospital single room & 1 heated mannequin	Hospital double room & 2 heated mannequins	Hospital double room, 2 heated mannequins & partition between beds.
Aerosol release	Room centre	Patient head	Patient 1 Patient 2	Patient 1 Patient 2

2.3. Sampling methodologies

All biological samples were taken on Tryptone soya agar (Oxoid, UK) as the controlled chamber conditions meant that no other species were present. Deposition was measured using settle plates located on the floor or on surfaces in the room. Given the inherent variability of biological particle collection, it was found that

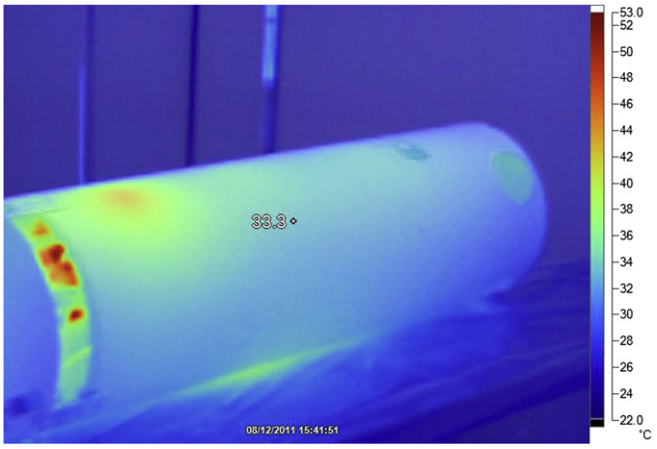

Fig. 2. Typical DIN man thermal output (°C).

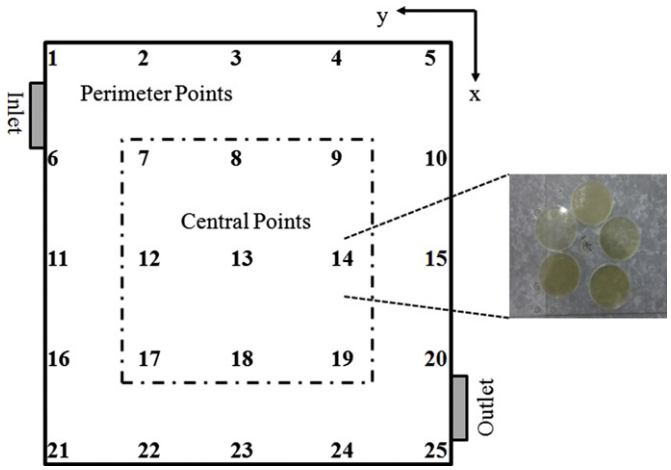

Fig. 3. Location of settle plates in the empty chamber scenario with photograph showing a sampling point with a typical group of five plates (scenario 1).

experiments carried out with fewer than 5 settle plates at each point yielded inconsistent results ($p \sim 0.1$). Electrostatic effects of aerosolisation were deemed to be negligible because of isotropic distribution of settle plates used for collection.

Scenario 1: Five 90 mm Petri dishes containing the growth media were placed at each enumerated position as shown in Fig. 3 with a total of 125 plates.

Scenarios 2–4: Petri-dishes were placed on furniture surfaces as indicated in Figs. 4 and 5. A minimum of seven plates were located at each position. Floor deposition was not measured in these cases.

Following experiments, the covered Petri-dishes were incubated for 24 h at 37 °C. Individual colony forming units (cfu) were then counted and recorded. All samples were subjected to minimal viable count threshold and those with less than 25 cfu per plate were discarded ($n = 3$).

Throughout all experiments particle concentrations (particle sizes 0.5–1 μm, 1–3 μm, 3–5 μm) were monitored at the outlet via a laser particle counter (at 2.83 L min^{-1}, Kanomax 3886 Optical Sciences Ltd, UK) to ensure steady state conditions were reached.

2.4. Data analysis

Sample size is small in all cases and since parametric statistics are notoriously sensitive to outliers, non-parametric statistical inference was used. The Wilcoxon rank-sum test was therefore used to compare experimental samples against CFD predictions. Comparison was made based on the null hypothesis of both samples stemming from distributions with equal variances, or more strictly that two independent samples emanate from the same distribution.

In all four study scenarios the environmental conditions remain reasonably constant, but variation is encountered within the biological organisms in use. In particular it is difficult to ensure that the injected concentration remains the same in different experiments. It is also difficult to directly relate the concentration in the nebuliser to the concentration measured on surfaces as there will be bacteria die off both in the nebulisation process and through loss of viability once in the room; neither factor is easy to measure. The study therefore focused solely on the relative spatial deposition in the room. As all experiments were conducted under comparable environmental conditions and all had the same duration, it was assumed that the rate of bacteria die off was the same throughout the room (a reasonable assumption) then it is possible to use a normalisation metric to ensure comparability of results between

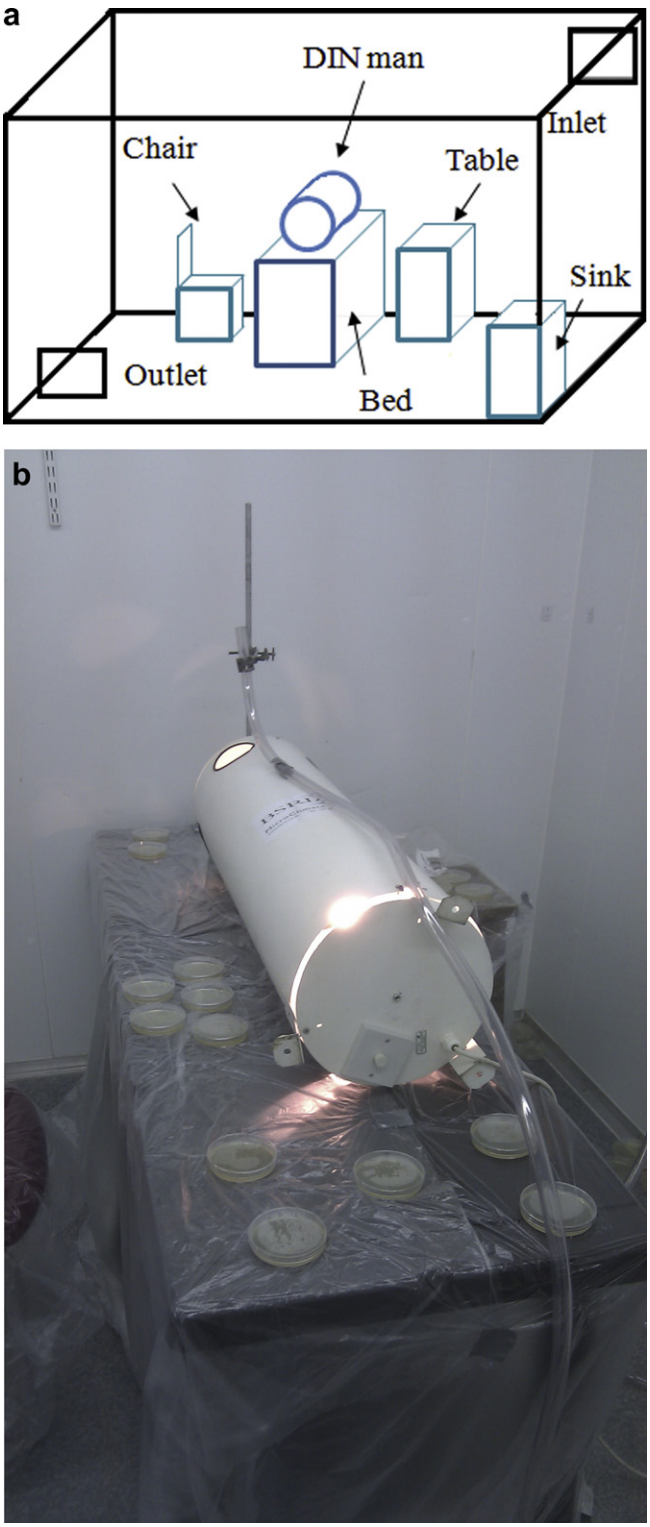

Fig. 4. Single-bed room experimental setup. Petri dishes were located on surfaces representing the bed, chair, table and sink. (a) Single-bed room schematic. (b) DIN man and petri dishes around bed.

experiments. In each case a fractional bacteria count C_i was determined to represent the normalised deposition distributions at each location. Values from colony counting were averaged based on the number of petri dishes at each point giving raw spatial counts, i.e. the average cfu count at each location is divided by the experimental average. This can be described by the following formula:

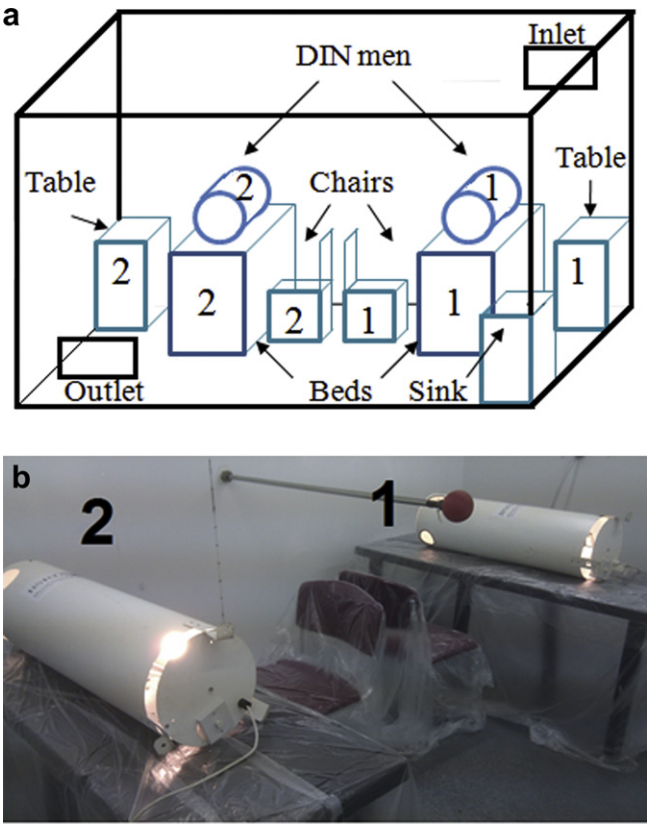

Fig. 5. Double-bed room experimental setup petri dishes were located on surfaces representing the bed, chair and table for each patient and the sink. (a) Double-bed room schematic. (b) DIN men enumeration: patient 1 and patient 2.

$$C_i = \frac{\frac{1}{m}\sum_{j=1}^{m} c_{ij}}{\frac{1}{m^*n}\sum_i \sum_j c_{ij}} \quad (1)$$

where n is the number of zones and m is the total number of Petri dishes in each zone.

Each positional value was then divided by the global mean of the experiment. Although scenarios were conducted on different days and using different microorganism cultures it was found that the mean values within each experiment scenario remained constant ($p = 0.3$). This therefore allows for quantitative as well as qualitative comparison between scenarios. A comparable normalisation approach was adopted in analysing simulation results to enable direct comparison between CFD and experimental spatial deposition patterns.

3. CFD methodology

Steady-state CFD models of the four experimental scenarios were developed using Fluent (ANSYS, version 12.0). Flow was simulated using a Reynolds' Average Navier–Stokes (RANS) approach, the most widely used method for indoor airflow [28–33]. A velocity profile was defined at the supply air diffuser, based on anemometry measurements (Fig. 1) and the extract was modelled as a negative pressure outlet (−25 Pa) on the boundary. An isothermal assumption was applied in the empty room simulation (scenario 1), while the hospital room scenarios (scenarios 2–4) applied a heat load of 35 W/m^2 on the DIN man. The Grashof/Reynolds's ratio indicates strong convective secondary flows and hence the energy equation was solved using the Boussinesq approximation in the latter cases. Fluent's standard air material $\rho = 1.225$ kg m^{-3}, $\mu = 1.84 \times 10^{-5}$ ns m^{-2} was used for the continuous phase.

As the focus of the simulations was on prediction of particle deposition, the resolution of turbulence, particularly close to the wall is important. RANS solutions of bulk-flow do not calculate turbulent fluctuations up to the wall, hence high Reynolds flows employ wall-functions and therefore an amalgamation of approaches is made. Enhanced wall functions rely on splitting the boundary region into two layers forcing unrealistic mesh sizes in some situations. Therefore Fluent's 'standard wall function' was employed, requiring the y^+ value to be within 30 and 300 in the first cell.

Previous studies have focused on small scale channel flow such as in the case described in Lai and Nazaroff [34]. Over-prediction of deposition quantities has been found when using the standard k–ε due to its Boussinesq modelling of isotropic Reynolds' stresses, worsening predictions close to the wall. Ideally all Reynolds' stresses are calculated individually as in the case of the RSM model. Although Wong et al. [18] found good comparison using the RNG k–ε model, other studies have found that improvement achieved over standard k–ε models, still show significant differences compared to empirically measured DNS data [36]. In order to explore further the influence of turbulence models to particle deposition in indoor air, both the RNG k–ε and the Reynolds' Stresses models are applied in this study.

3.1. Bioaerosol simulation

Lagrangian Particle tracking with stochastic discrete random walk (DRW) was used to represent the eddy interactions of the discrete phase. Bioaerosols were simulated as spherical water droplets, 2.5 μm in diameter. The mean mass size of droplets was based on knowledge of the Collison nebuliser, although it was found that particles between 1 and 5 μm yielded similar results. The presence of microorganisms in the diluted aerosolised solution was assumed to have a minimal influence on droplet density. Particle trajectories are calculated by a fifth order Runge–Kutta method by considering the change in particle velocity u_i^p due to drag force, inertia $(u_i - u_i^p)$, gravity g_i, lift force F_i^L and Brownian motion $n_i(t)$ thus:

$$\frac{du_i^p}{dt} = \frac{1}{\tau}\frac{C_D Re_P}{24}\left(u_i - u_i^p\right) + g_i + F_i^L + n_i(t) \quad (2)$$

where τ is the particle relaxation time given by:

$$\tau = \frac{Sd^2 C_c}{18\nu} \quad (3)$$

where, S is the particle-fluid density ratio, d the particle diameter, ν the fluid kinematic viscosity and C_c is the Cunningham–Stokes slip correction factor given by:

$$C_c = 1 + \frac{2\lambda}{d}\left(1.257 + 0.4e^{-\left(\frac{1.1d}{2\lambda}\right)}\right), \quad (4)$$

where λ = gas molecular mean free path.

Particles representing bioaerosols were released from source locations comparable to the experimental study. The *S. aureus* suspension in scenario 1 is released from the centre of the chamber isotropically by means of a sphere containing 12 holes. In the CFD

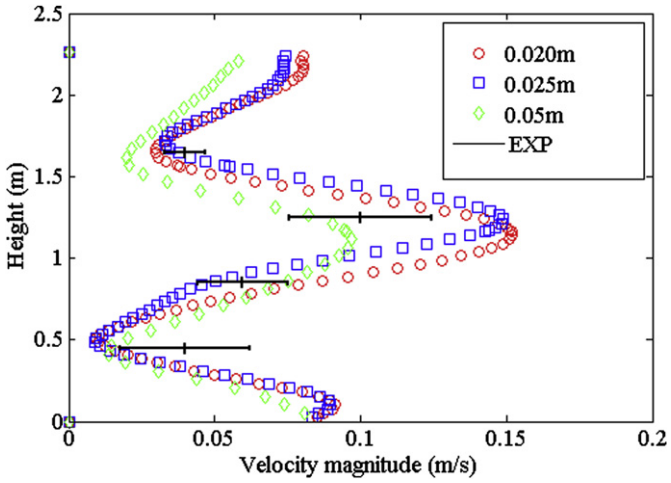

Fig. 6. Sensitivity of velocity to grid for three meshes at pole 2 (see Fig. 7a).

model particles were injected from a comparable volume at the centre of the room. A sensitivity study showed that applying a momentum source to the particles within the CFD release did not make any significant difference to deposition patterns.

Experimental release of bioaerosols in scenarios 2–4 was via a tube placed at the head of the mannequin, pointing vertically upwards to represent a respiratory release and held in place by a clamp to ensure no movement. The CFD model simulated this through release from a small volume at an equivalent location. Although a directed momentum source equivalent to the inlet velocity was defined in this case, it had a negligible effect as the particle trajectory was dominated by the effect of the thermal plume. Therefore it was found that although the release location influenced the simulation results, the way in which particles were released did not have a significant effect.

Compared to the bulk-flow in the chamber, particle contribution to density was considered sufficiently low and therefore only one-way turbulence interaction was employed.

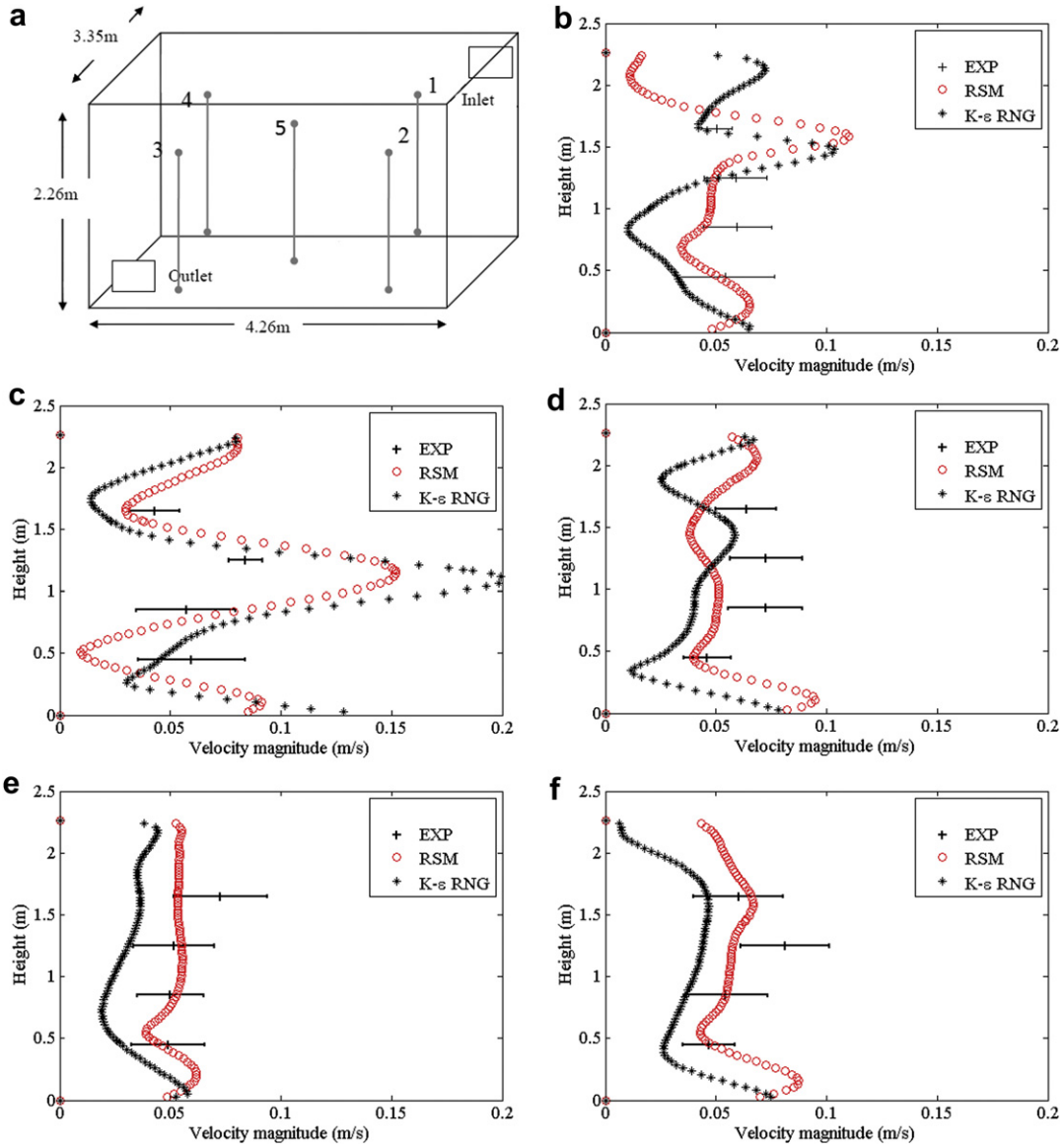

Fig. 7. Anemometry comparison against $k-\varepsilon$ RNG and RSM turbulence models for the empty chamber (scenario 1). (a) Measurement positions. (b) Anemometry at position 1. (c) Anemometry at position 2. (d) Anemometry at position 3. (e) Anemometry at position 4. (f) Anemometry at position 5.

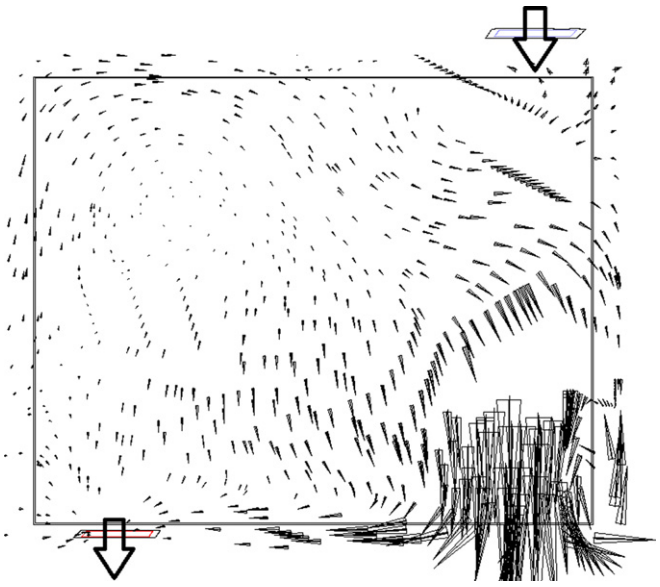

Fig. 8. Simulated velocity vectors on a horizontal plane at a height of 1.2 m.

3.2. Grid sensitivity

Grid density and construction has been shown to influence flow results heavily [32,35,37,38] therefore a mesh independence study was first undertaken for the empty room scenario. Three hexahedral grids were compared with nominal cell sizes of 50 mm, 25 mm, and 20 mm. Velocity variation was found to differ less than 5% between the 25 mm and 20 mm meshes as shown in Fig. 6.

Bulk flow was calculated using the SIMPLE algorithm with the second order upwind scheme for all variables. Roache [37] suggests that often velocity grid independence may be reached prematurely with respect to particle tracking, since large disparity must exist between cell size and particle diameter. Therefore, particle tracking length scale was increased to reflect at least five calculations per cell. Particle count independence was achieved at particle numbers above 50,000 and little significant improvement was gained thereafter. Final mesh size was in the region of 4 million cells for all four scenarios.

4. Results

4.1. Scenario 1: empty room

Simulated velocity magnitudes at five vertical locations are presented in Fig. 7 and compared to experimental data from anemometry readings at 4 points in each location. These measurements were recorded during a prolonged period of steady airflow and in each case show the mean and standard deviation over a 20 min measurement period. Despite some variability in the measured data, both the $k-\varepsilon$ RNG and RSM turbulence model simulations capture the main features of the flow well. The data clearly indicates spatial variability in the chamber airflow. In the breathing zone ($y = 1.6$ m), the velocity profiles at poles 1 and 2 are generally higher due to the impinging jet from the inlet diffuser while velocities in the region of pole 4 are generally lower. A vector plot of the simulated airflow with the RSM turbulence model (Fig. 8) shows these lower velocities correspond to slow recirculation in this region.

Normalised experimental deposition values are presented together with numerical predictions from the RSM and $k-\varepsilon$ RNG turbulence models at the central nine points within the empty room in Fig. 9(a). Scatter plots comparing the numerical results with experimental averages at all 25 points are presented for both turbulence models in Fig. 9. As shown by Fig. 9(a), the measured deposition in the nine zones directly below the source is fairly uniform with normalised reported values between 0.82 and 1.62 Relatively little variance was found here. Comparison with the simulation results shows the RSM model more accurately corresponds to experimental data ($r = 0.93$, $p = 0.59$), however $k-\varepsilon$ RNG does not perform poorly ($r = 0.63$, $p = 0.29$) in this region. Zones around the perimeter of the room showed more sizable scatter with normalised deposition down to 0.69 and show less good comparison with the CFD models, with correlation coefficients of $r = 0.27$ and $r = 0.86$ for the RSM and $k-\varepsilon$ RNG, respectively. The $k-\varepsilon$ model simulation tends to predict a more uniform deposition, with an agglomeration around the mean (Fig. 9c). However the calculations of anisotropic Reynolds stresses under the RSM model produces a tighter relationship and hence makes an improved comparison ($r = 0.95$). Both models tend to over-predict low deposition and under-predict high deposition, but this is found to a greater extent with the $k-\varepsilon$ model. This is indicated in the lines of best fit and also in both data sets displaying a weak right skew.

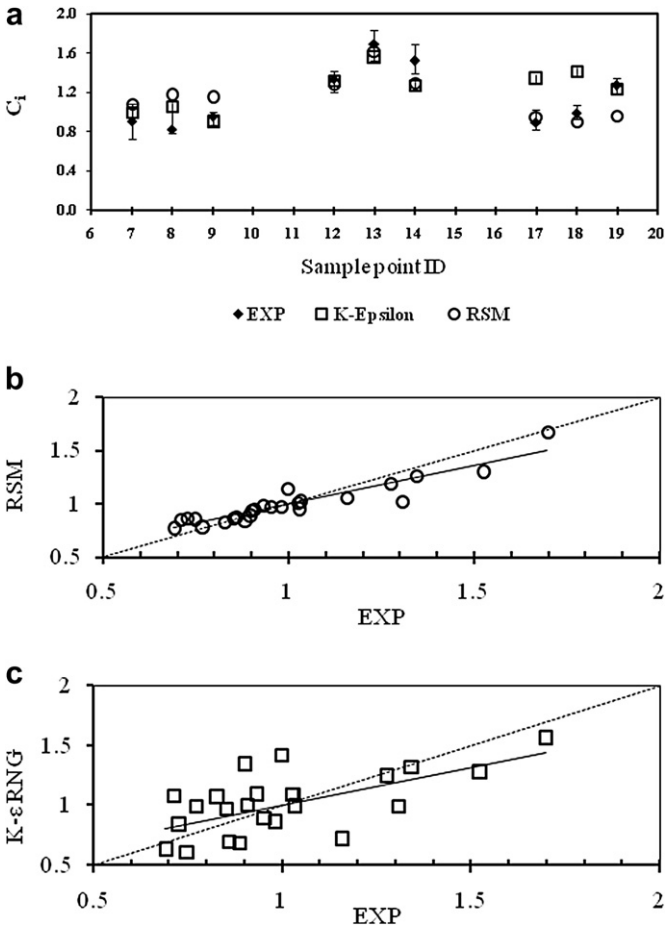

Fig. 9. Comparison between experimental data and numerical deposition predicted by the two turbulence models. (a) Comparison with both turbulence models at nine central points in the empty room (Fig. 3). (b) Correlation between experimental data and RSM turbulence model results at all 25 sample points. (c) Correlation between experimental data and $k-\varepsilon$ RNG turbulence model results at all 25 sample points.

4.2. Scenario 2: single patient room

Fig. 10 shows simulated temperature contours and velocity vectors for the single patient room, plotted on the horizontal

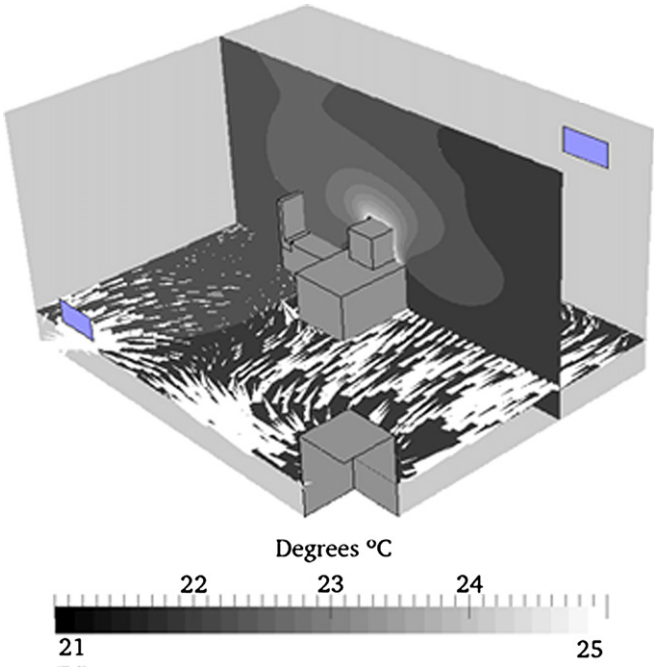

Fig. 10. Temperature contours in single room overlaid with velocity magnitude vectors.

surface through the bed. Complex flow structures can be observed, with the cold inlet air impinging on the opposite wall and multiple recirculation zones at the foot of the bed. A vertical heat plume emanates from the supine mannequin and is depicted in the vertical plane. In reality, such a strong human heat plume may not be observed in non-quiescent conditions [39], however other heat sources such as lighting or medical equipment may add to the load.

Normalised experimental deposition on the four horizontal furniture surfaces is compared to simulation results with two turbulence models in Fig. 11. While Fig. 10 shows the flow in this situation is less homogeneous than the empty room, the experimentally measured deposition still remains relatively uniform with mean normalised values between 0.64 and 1.16 on the four surfaces. Although the bioaerosol source was located at the patient head, deposition on the bed is lower than other surfaces which may be due to the convective plumes above the DIN-man promoting transport away from the source. The highest measured deposition is on the surface representing a sink, despite this being the furthest location from the source. While both turbulence models predict the same spatial trends as the experiments, the $k-\varepsilon$ model has a greater tendency to over or under predict in this case, with only one of the four locations showing a good comparison with the experimental result. However the RSM model shows very good comparison with the experimental results, with similar magnitude deposition as

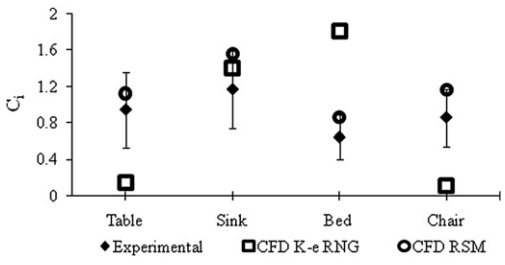

Fig. 11. Comparison between numerical and experimental deposition on furniture surfaces in the single patient room.

well as spatial distribution with a small but consistent tendency to over-predict.

4.3. Scenarios 3 and 4: double patient room

The double-bed room experimental setup was designed to test two main scenarios: influence of a partition and influence of the airflow. The influence of the airflow is considered by switching the location of the infectious source from patient 1 to patient 2 Comparison between scenario 3 and 4 therefore allows for observation of the effect of a partial partition and also the extent to which the fresh supply air above patient 1 influences deposition in that and the neighbouring bed bay. In scenario 4, where a partial partition is required, a plastic sheet was hung between the patients such that it provided a physical barrier between beds. Gaps of 20 cm were left at the top and the bottom of the sheet as well as 80 cm at the end of the beds to allow for healthcare worker passage. In experiments investigating scenarios 3 and 4 bioaerosol deposition was measured through 9 Petri dishes located on surfaces representing the chair, sink and bedside table for each patient respectively. Due to the large area of the bed, this was covered by 15 dishes to avoid the effect of spatial variation.

Fig. 12 shows velocity magnitude contours and velocity vectors for scenarios 3 and 4. In the case with no partition the air velocities tend to be similar close to both patients (Fig. 12a). The directional arrows indicate a tendency for air movement from patient 1 to patient 2 on the way to the outlet. The partition however creates a physical barrier thereby streamlining the flow towards the extract (Fig. 12b) and reducing the velocity magnitude in the region of patient 2.

Fig. 13 depicts the normalised experimental results at each patient surface group for scenarios 3 and 4 based on the source of bioaerosols. When patient 1, lying directly beneath the supply air vent, is the bioaerosol source (Fig. 12a) the partition has a negligible effect on the deposition onto the infectious patient surface group (Table 1, bed 1 and chair 1). However, the partition does influence the deposition on the surface group for patient two. In the absence of a partition, bed 2 becomes the main destination surface for particles released at patient 1, surpassing that of the own infectious patient. A significant decrease is apparent at this point and other surfaces around patient 2 when the partition is installed, although the deposition is still a similar magnitude to that around patient 1. It is also noticeable that in both cases with patient 1 as the source, there is greater spatial variation in the deposition pattern than for any other scenarios studied in this paper.

Fig. 13b reverses the source position, where now the infectious point becomes patient 2. Statistically there appears to be no significant difference between the distributions, where the null hypothesis of equal medians cannot be rejected at the 5% level. However a tendency of higher deposition on bed and chair 2, which are closer to the partition, can be observed. This could be in part explained by the plume from the patient 2 tending to drift towards the partition and hence towards chair 2 (see Fig. 11b). In contrast patient 1's particle release plume is quickly dispersed and overwhelmed by the incoming faster air.

To further explore the influence of the partition univariate linear regression was carried out between the data sets, where the only dependent variable was the normalised deposition count. In the case where patient 1 is the source a two-fold reduction in pathogen deposition per surface can be predicted ($r = -0.32$, $p = 0.0254$) for patient 2 between scenarios 3a and 4a. Reduction in the second case, when the pathogen source is situated directly opposite the extract vent, is however negligible.

Comparison of the experimental deposition patterns with CFD simulations are presented in Fig. 14 for scenarios 3 and 4 with both

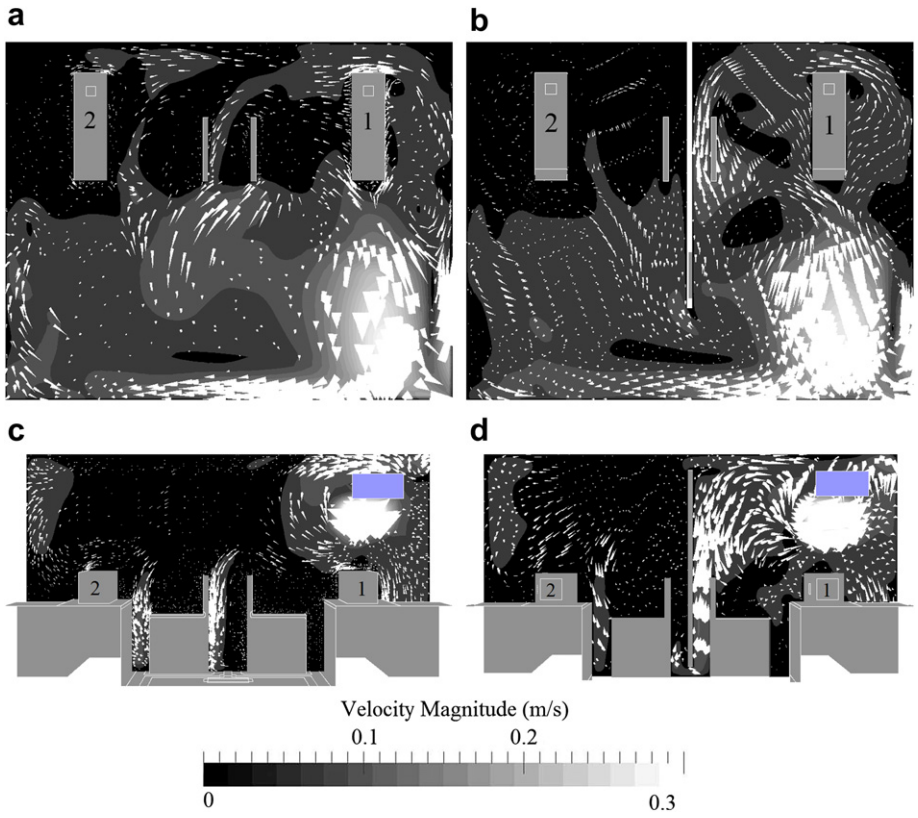

Fig. 12. CFD velocity magnitude contours showing airflow patterns present in all double-bed room scenarios: scenario 3 without (a and c) and scenario 4 with (b and d) a partial partition. (a) No partition, horizontal plane $z = 1$ m. (b) With partition, horizontal plane $z = 1$ m. (c) No partition, vertical plane $y = 2.4$ m. (d) With partition, vertical plane $y = 2.4$ m.

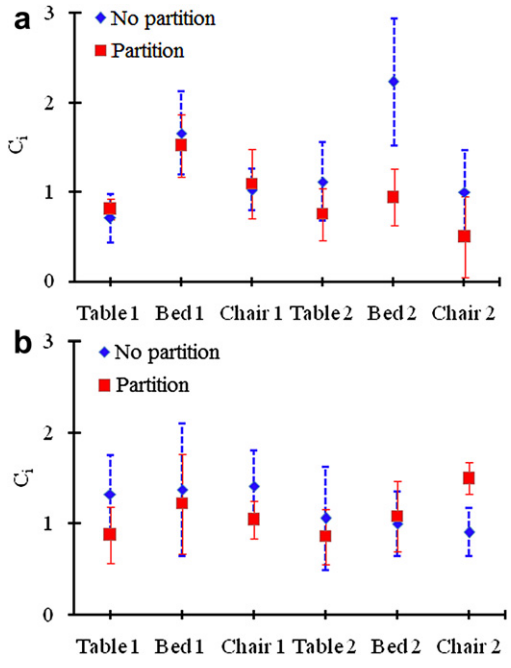

Fig. 13. Influence of partition and source location on experimentally measured deposition. a) Comparison of normalised values for colony counting based on release from patient 1, scenarios 3a (no partition) and 4a (with partition). b) Comparison of normalised values for colony counting based on release from patient 2, scenarios 3b (no partition) and 4b (with partition).

patients as the source. In all cases, both models give a reasonable prediction with only a small number of locations, notably the values at bed 2 in Fig. 13a and Table 1 in Fig. 13b, where the CFD simulations compare poorly with the experimental results. There is noticeably more variation in these scenarios, with less clear differentiation between the results produced by the two turbulence models. Generally the predictions are closer to the experimental data nearer to the source with the RSM model giving slightly better results. This is also evident in the correlation coefficients presented in Table 2.

5. Discussion

It is desirable to be able to produce realistic simulations of bioaerosol deposition in indoor environments to aid design and risk assessment, yet there is little previous work to evaluate the reliability of CFD predictions. The results presented here suggest that it is viable to use CFD to predict realistic spatial deposition of small particle bioaerosols and hence makes an important step in validating the use of CFD techniques for modelling bioaerosol behaviour in indoor environments.

5.1. Scenario 1: empty chamber

The first scenario represents a controlled condition to ensure that experimental scenarios are directly comparable to idealised numerical scenarios. Due to the physical dimensions of the anemometer protective cage there were some restrictions of the distance from the wall at which the flow could be measured. However it is clear that CFD is capable of representing the bulk flow field within the chamber to a high degree. Indoor air patterns are inherently variable but the CFD models using both RSM and $k-\varepsilon$

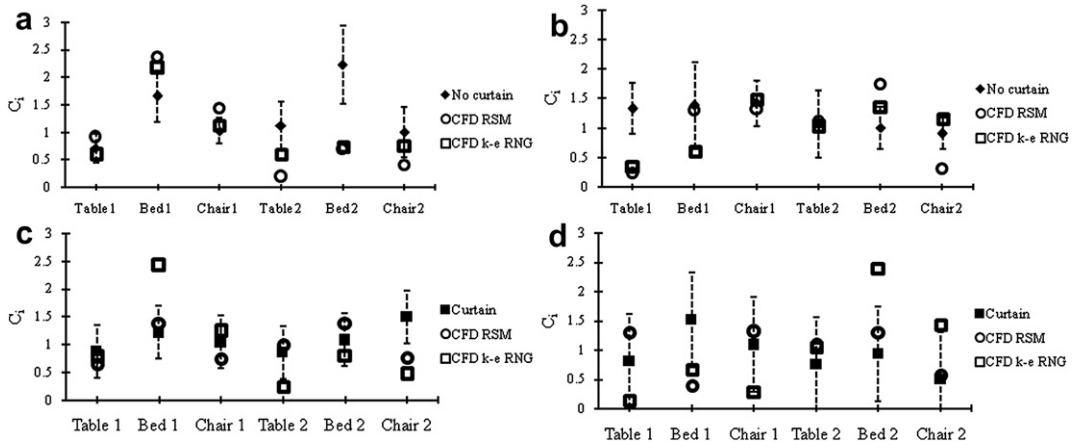

Fig. 14. Normalised CFD compared to experimental deposition for scenarios 3 and 4. a) Scenario 3a: infectious patient = 1, susceptible patient = 2. b) Scenario 3b: infectious patient = 2, susceptible patient = 1. c) Scenario 4a: infectious patient = 1, susceptible patient = 2. d) Scenario 4b: infectious patient = 2, susceptible patient = 1.

RNG turbulence models predict reasonable characterisations. Nevertheless the anisotropic turbulence model generally makes an improvement over the eddy viscosity assumption model, particularly in the regions of higher shear and velocity gradients. Lai and Nazaroff [34] suggest that the inclusion of the effect of turbophoresis may enhance particle deposition, particularly where the vertical turbulence gradient is high close to the wall.

Experience from the current study shows that a minimum of five settle plates are needed at each collection point to achieve a statistically reliable and replicable result. Bioaerosol deposition comparisons tended to be well predicted by both turbulence models in the central regions, but accuracy deteriorated towards the outer edges of the room, particularly in the cases using $k-\varepsilon$ RNG. The prevalence of homogeneity in turbulence appears to translate to particle depositions, particularly for size ranges where body forces dominate [17]. The Reynolds' Stress turbulence model allowed anisotropic flow patterns to be adequately captured, leading to a very strong comparison between spatial depositions. In addition only minor variations were observed in the CFD prediction, given particle number independence, which is reflected in the high r value of the linear polynomial fit.

Overall the results suggest slightly higher deposition close to the source, possibly due to the largest particles dropping out of the air before evaporating. However deposition is apparent across the room indicating the combined influence of air movement and gravitational settling on the small diameter particles.

5.2. Scenario 2: single-bed room

The second scenario considered adds both complexity and realism by including key items of furniture plus a DIN-man to take into account the heat plume generated by a quiescent resting patient in a hospital single-bed room. Spatial variation in deposition was compared between important furniture surfaces including the bed, bedside table and visitor's chair. A stronger heterogeneity was observed here in comparison to the empty chamber, mainly due to the modified flow gradients imposed by furniture and the convective heat plume. Due most probably to the latter, the patient's bed showed lower deposition quantities in comparison to neighbouring surfaces. While this gives some insight into the potential influence of the thermal plume in transporting bioaerosol particles away from the source, the results must be interpreted with caution. In reality the patient may not be permanently facing upwards and would likely move during their sleep. Additionally, bed clothes are usually present on hospital beds, producing a larger surface area on which particles may be trapped. While the assumption of a steady state simulation and experimental set-up is considered suitable for evaluating the constant release of pathogens from a breathing patient, this is unlikely to be appropriate for situations where doctors and nurses are disturbing the airflow patterns by opening doors or shaking bed clothes, creating inherently transient airflow patterns. Despite the simplifications, it is worth noting that, as in the empty room scenario, the experiments and simulations both show measurable deposition across the room space clearly indicating the ability for a bioaerosol source to result in environmental contamination at some distance from the source.

Table 2
Statistical analysis of correlation between experimental deposition and CFD for scenarios 3 and 4.

	Infectious patient	Scenario 3		Scenario	
		3a	3b	4a	4b
		1	2	1	2
$k-\varepsilon$ RNG model	p-value	0.46	0.67	0.13	0.81
	Correlation coefficient (r)	0.23	0.2	0.35	0.94
RSM model	p-value	0.48	0.7	0.93	0.59
	Correlation coefficient (r)	0.8	0.2	0.55	0.43

In terms of numerical comparison, the $k-\varepsilon$ turbulence model simulation at best predicts normalised particle deposition values within one standard deviation of experimental findings. In particular, both the bedside table and the chair have almost zero predicted deposition values. RSM on the other hand appears to slightly overpredict deposition in all cases, but remains within one standard deviation of the experimental results. The latter result is supported by previous conclusions for numerical simulation of particle depositions in pipes [42]. While comparison for both turbulence models shows a lower agreement than the empty room scenario, this is not unexpected. The addition of a significant heat source and furniture adds complexity and hence uncertainty to the CFD model. It is necessary to simplify the geometries of furniture and the DIN man in the model, which will have some effect on the solution accuracy. Similarly the bioaerosol release location cannot be as accurately defined compared to the empty room model which again may influence the results.

5.3. Scenarios 3–4: double-bed room

UK hospitals were historically constructed with multi-bed wards as the primary form of patient accommodation and this

remains the case in the majority of hospitals. The results from the final stage of this study give some insight into the potential for cross-transmission of infection between patients due to deposition of pathogenic aerosol particles on key surfaces. As with the two previous scenarios, both experiments and simulations demonstrated that a bioaerosol release in both an open (scenario 3) and partitioned (scenario 4) room can result in measurable surface contamination across the whole of the room space. Of particular interest was the effect of both the location of the infectious source with respect to the inlet diffuser and the level of protection that a partition provides in terms of surface deposition in the neighbouring cubicle. When the source patient is located directly under the inlet vent (cubicle 1) the partition proved effective at limiting the deposition in the neighbouring cubicle (Fig. 12a). However the partition's influence appears to be quite sensitive to reversing the source location (Fig. 12b). In the latter case particle deposition proved more homogeneous and hence the partition played a secondary role to the effect of ventilation inlet position. As noted during the CFD and anemometry measurements, cubicle 2 provides areas of very slow moving air and consequently probable recirculation pockets. Therefore these allow particles to be dispersed towards cubicle 1 as well as being extracted. As a corollary, positioning the susceptible patient upwind of the infectious source (in our case in cubicle 1) also results in a significant reduction in risk. The effectiveness of the partition is also likely related to its particular deployment in the form of a curtain with gaps above and below. However during a common diurnal hospital scene most curtains are usually only half drawn or fully retracted. In addition to this, and mainly to aid in cleaning, they often hang approximately 20 cm from the ground and a similar distance from the ceiling. Consequently this space exposes a gap for potential passage of pathogens, increasing cross transfer susceptibility. Previous numerical simulations have shown that full height partitions may reduce airborne transmission risk [26] and that those curtaining the length of patient beds are more effective than partially extended ones at preventing infection [40,41]. Physical barriers clearly point to effective intervention measures however further evaluation is needed to explore the most appropriate design and the limitations of such an approach.

CFD comparison concurred with the findings from the two previous scenarios. The further increase in complexity in the two-bed case again led to more variation in the CFD solutions. As previously shown, the RSM model generally led to better predicted deposition than the $k-\varepsilon$ RNG model, although both models produced realistic deposition patterns. Simulations suggested that particles released from patient 2 were drawn towards the inlet jet, probably due to the regions of low pressure created by the faster moving air. This effect dominated the simulations where a partial partition was absent and to a lesser effect when one was present.

5.4. Implications of results

Across all scenarios it is noted that both experiments and simulations predict measurable deposition across the room space. While spatial variation depends on layout, the results suggest there is clear potential for small diameter ($\sim$2.5 μm) particles to play a role in transmission of infection through indirect contact routes. This is an important consideration; such particles are routinely regarded as airborne and hence controlled through ventilation rather than cleaning. Moreover, these small particles are usually only considered of concern where the pathogen is classed as possibly capable of direct airborne transmission, for example tuberculosis, measles or influenza. The deposition of culturable bioaerosols in this study adds support to the hypothesis that airborne dispersion may play a role in non-respiratory infections such as MRSA and *Clostridium difficile* [23,27], with surface contamination and subsequent contact by susceptible people resulting in transmission.

The study conducted here demonstrates the potential for CFD simulations to accurately predict the relative spatial distribution of bioaerosol deposition, but it has not been possible to confirm whether simulations can predict the actual level of contamination based on a particular amount released into the space. The reason for this lies in the limitations of the experimental methods. To relate the deposition to the bioaerosol concentration in the air requires taking air samples. While this is straightforward [17], it is well documented that sampler efficiencies are far from 100%, with some estimated to sample well below 50% of the viable concentration in the air [43]. The settle plate approach used to measure deposition is unlikely to experience microbial losses due to physical damage from impaction that is present in an air sampler, but may still underestimate total counts as it is based on colony formation after incubation. As the surface deposition and air samples must be measured using different techniques, neither of which has a well characterised sampling efficiency, it is not feasible to quantitatively relate the results from the two approaches. It is for this reason that biological air sampling was not conducted in this study.

The CFD solutions may benefit in future from the use of a low-Reynolds' turbulence model instead of the logarithmic law utilised with both turbulence models tested. Given the exclusion of the effect of turbophoresis, the DRW model provides extra impetus to deposition velocities. In some cases this may be unphysically large, which probably accounts for some of the over-deposition observed. However computational costs would still be unreasonable due to the level of grid resolution required.

The Reynolds' Stress model used in this study requires greater care during pre-processing and initially defining the geometry and mesh than the empirically based $k-\varepsilon$ model. It was found that small fascia such as a patient's mouth proved a source of instability when utilising the second order spatial discretisation scheme and hence these should be replaced by appropriate energy and momentum sources. Implications for convergence and computational resources are also considerable however substantially lower than those required for a transient LES simulation. Ultimately a physically realistic solution can nevertheless be obtained.

6. Conclusions

This study provides a direct room-scale comparison between CFD simulations and experimental bioaerosol deposition under idealised but realistic single and two-bed room scenarios. The results have demonstrated the following:

- A good comparison is possible between the spatial deposition patterns predicted through CFD simulation and those measured through experimentation. Comparison is improved by using an RSM turbulence model which correctly resolves the anisotropic nature of the flow compared to the $k-\varepsilon$ turbulence model that is applied in the majority of indoor air studies. It is recommended that when CFD is applied as a design tool, careful consideration should be given to which turbulence model is used particularly where particle deposition is considered.
- Common hospital ventilation guidelines consider that bioaerosols of diameters less than 5 μm are typically thought to be extracted by the ventilation regime before being deposited on surfaces. However this study shows that bioaerosol particles below 5 μm diameter do deposit on surfaces. The bioaerosols studied have shown to be deposited across all horizontal surfaces in a room, with surface concentration not clearly

related to distance from the bioaerosol source. This suggests that small pathogen carrying particles may play a role in the environmental contamination of hospital rooms and hence the risk of indirect contact transmission. Hospital studies have shown that bedside tables are both high contact nodes for healthcare workers [44] and are also proven to exhibit contact transmission probabilities of at least 1 in 5 [45]. Deposition onto such surfaces may therefore be important in some situations and may have implications for nursing practices or frequency of cleaning procedures.

- The spatial deposition of particles is influenced by the location of the ventilation supply inlet relative to the source. Locating a susceptible patient closer to the supply air and introducing a partition between beds are both likely to reduce the risk of environmental contamination due to bioaerosol release from a neighbouring patient. This finding concurs with tracer gas and simulation based studies evaluating airborne infection risk [13,26]

Acknowledgements

This work was carried out as part of a PhD studentship supported by the UK Engineering and Physical Sciences Research Council (EPSRC) and Arup. The authors would like to thank Dr Louise Fletcher and Sheena Bennett for their assistance with the experimental work along with Dr Carl Gilkeson and Dr Amir Khan for CFD expertise and logistics.

References

[1] World Health Organization. WHO guidelines on hand hygiene in health care. Technical report; 2009.
[2] Klevens RM, Edwards JR, Richards CL. Estimating health-care associated infections and deaths in U.S. hospitals. Public Health Rep 2002;122.
[3] Harbarth S, Sax H, Gastmeier P. The preventable proportion of nosocomial infections: an overview of published reports. J Hosp Infect 2003;54:258–66.
[4] Hathway EA. CFD modelling of pathogen transport due to human activity. PhD thesis: Civil Engineering, University of Leeds; 2008.
[5] Roberts K, Hathway EA, Fletcher LA, Beggs CB, Elliot MW, Sleigh PA. Bioaerosol production on a respiratory ward. Indoor Built Environ 2006;15:35–40.
[6] Boswell TC, Fox PC. Reduction in MRSA environmental contamination with a portable HEPA-filtration unit. J Hosp Infect 2006;63(1):47–54.
[7] Dancer SJ. Mopping up hospital infection. J Hosp Infect 1999;43:85–100.
[8] Otter JA, Yezli S, French GL. The role played by contaminated surfaces in the transmission of nosocomial pathogens. Infect Control Hosp Epidemiol 2011; 32(7):687–99.
[9] Rusin P, Maxwell S, Gerba C. Comparative surface-to-hand and fingertip-to-mouth transfer efficiency of gram-positive bacteria, gram-negative bacteria and phage. J Appl Microbiol 2002;93:585–92.
[10] Ayliffe GAJ, Fraise AP, Geddes AM, Mitchell K. Control of hospital infection: a practical handbook. 4th ed. London: Arnold; 2000.
[11] Rutala WA, Katz EB, Sherertz RJ, Sarrubi Jr FA. Environmental study of a methicillin-resistant *Staphylococcus aureus* epidemic in a burn unit. J Clin Microbiol 1983;18(3):683.
[12] Xie X. Evaporation and movement of respiratory droplets in indoor environments. PhD thesis: The University of Hong Kong; 2008.
[13] Qian H, Li Y, Nielsen PV, Hyldgaard CE, Wong TW, Chwang ATY. Dispersion of exhaled droplet nuclei in a two-bed hospital ward with three different ventilation systems. Indoor Air 2006;16(2):111–28.
[14] Tian ZF, Tu JY, Yeoh GH, Yuen RKK. On the numerical study of contaminant particle concentration in indoor airflow. Building Environ 2006;41:1504–14.
[15] Zoon WAC, Loomans MGLC, Hensen JLM. Testing the effectiveness of operating room ventilation with regard to removal of airborne bacteria. Building Environ 2011;46(12):2050–77.
[16] Tian L, Ahmadi G. Particle deposition in turbulent duct flows – comparisons of different model predictions. J Aerosol Sci 2007;38:377–97.
[17] Hathway EA, Noakes CJ, Sleigh PA, Fletcher LA. CFD simulation of airborne pathogen transport due to human activities. Building Environ 2011;46(12): 2500–11.
[18] Wong LT, Chan WY, Mui KW, Lai ACK. An experimental and numerical study on deposition of bioaerosols in a scaled chamber. Aerosol Sci Technol 2010; 44(2):117–28.
[19] Lai ACK, Chen F. Modelling particle deposition and distribution in a chamber with a two-equation Reynolds-averaged Navier–Stokes model. J Aerosol Sci 2006;37:1770–80.
[20] Chen Q, Jiang Z, Moser A. Control of airborne particle concentration and draught risk in an operating room. Indoor Air 1992;2(3):154–67.
[21] Kibbler CC, Quick A, O'Neill AM. The effect of increased bed numbers on MRSA transmission in acute medical wards. J Hosp Infect 1998;39:213–9.
[22] Sheretz RJ, Reagan DR, Hampton KD, Robertson KL, Streed SA, Hoen HM, et al. A cloud adult: the *Staphylococcus aureus* virus-interaction revisited. Ann Intern Med 1996;124(6):539–47.
[23] Noakes CJ, Sleigh PA, Escombe AR, Beggs CB. Use of CFD analysis in modifying a TB ward in Lima, Peru. Indoor Built Environ 2005;15(1):41–7.
[24] Chaudhury H, Mahmood A, Valente M. Advantages and disadvantages of single-versus multiple-occupancy rooms in acute care environments: a review and analysis of the literature. Environ Behav 2005;37:760.
[25] Dettenkofer MS, Seegers S, Antes G, Motschall E, Schumacher M. Does the architecture of hospital facilities influence nosocomial infection rates? A systematic review. Infect Control Hosp Epidemiol 2004;25(1):21–5.
[26] Ulrich RS, Zimring C, Zhu X, DuBose J, Seo H-B, Choi Y-S, et al. A review of the research literature on evidence-based healthcare design. The Center for Health Design; 2008.
[27] Roberts K, Smith C, Snelling A, Kerr K, Banfield K, Sleigh PA, et al. Aerial dissemination of *Clostridium difficile spores*. BMC Infect Dis 2008;8:1–7.
[28] Chow TT, Yang XY. Performance of ventilation system in non-standard operating room. Building Environ 2003;38(12):1401–11.
[29] Zhang Z, Chen Q. Comparison of the Eulerian and Lagrangian methods for predicting particle transport in enclosed spaces. Atmos Environ 2007;41: 5236–48.
[30] Bjørn E, Nielsen PV. Dispersal of exhaled air and personal exposure in displacement ventilated rooms. Indoor Air 2002;12(3):147–64.
[31] Noakes CJ, Sleigh PA. Mathematical models for assessing the role of airflow on the risk of airborne infection in hospital wards. J R Soc Interf 2009;6:S791–800.
[32] Nielsen PV, Allard F, Awbi HB, Davidson L, Schälin A. CFD in ventilation design a new REHVA guide book. Aalborg University; 2009.
[33] Qian H, Li YG, Nielsen PV, Huang XH. Spatial distribution of infection risk of SARS transmission in a hospital ward. Building Environ 2009;44:1651–8.
[34] Lai ACK, Nazaroff WW. Modelling indoor particle deposition from turbulent flow onto smooth surfaces. J Aerosol Sci 2000;31(4):463–76.
[35] Li Y, Huang X, Yu ITS, Wong TW, Qian H. Role of air distribution in SARS transmission during the largest nosocomial outbreak in Hong Kong. Indoor Air 2005;15(2):83–95.
[36] Kim J, Moin P, Moser RD. Turbulent statistics in fully developed channel flow, at low Reynolds number. J Fluids Mech 1987;177:133–66.
[37] Roache PJ. Quantification of uncertainty in computational fluid dynamics. Annu Rev Fluid Mech 1999;29(123):60.
[38] Srebric J, Vukovic V, He G, Yang X. CFD boundary conditions for contaminant dispersion, heat transfer and airflow simulations around human occupants in indoor environments. Building Environ 2008;43(3):294–303.
[39] Tang JW, Noakes CJ, Nielsen PV, Eames I, Nicolle A, Li Y, et al. Observing and quantifying airflows in the infection control of aerosol and airborne-transmitted diseases: an overview of approaches. J Hosp Infect 2011;7: 213–22.
[40] Okell CC, Elliot SD. Cross-infection with haemolytic streptococci in oto-rhinological wards. The Lancet 1936;228(5902):836–42.
[41] Ching WH, Leung MKH, Leung DYC, Li Y. Reducing risk of airborne transmitted infection in hospitals by use of hospital curtains. Indoor Built Environ 2008; 17(3):252–9.
[42] Lach W. Performance of the surface air system air samplers. J Hosp Infect 1985;6:102–7.
[43] Dehbi A. A CFD model for particle dispersion in turbulent boundary layer flows. Nucl Eng Des 2008;238(3):707–15.
[44] Huslage K, Rutala WA, Sickbert-Bennett E, Weber DJ. A quantitative approach to defining "high-touch" surfaces in hospitals. Infect Control Hosp Epidemiol 2010;31(8):850–3.
[45] Hayden MK, Blom DW, Lyle EA, Moore CA, Weinstein DA. Risk of hand or glove contamination after contact with patients colonized with vancomycin-resistant enterococcus or the colonized patients' environment. Infect Control Hosp Epidemiol 2008;29(2):149–54.